Chaos, Solitons and Fractals 180 (2024) 114582

Contents lists available at ScienceDirect

Chaos, Solitons and Fractals

journal homepage: www.elsevier.com/locate/chaos

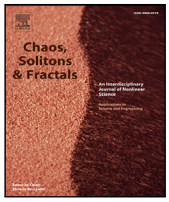

Dynamical instabilities cause extreme events in a theoretical Brusselator model

S.V. Manivelan [a], S. Sabarathinam [b,c], K. Thamilmaran [d], I. Manimehan [a,*]

[a] Department of Physics, M. R. Government Arts College (Affiliated to Bharathidasan University), Mannargudi, 614 001, Tamilnadu, India
[b] Department of Computational Biology, Saveetha School of Engineering, Saveetha Institute of Medical and Technical Sciences, Saveetha University, 602 105, Thandalam, Chennai, Tamil Nadu, India
[c] Laboratory of Complex Systems Modelling and Control, Faculty of Computer Science, National Research University, High School of Economics (HSE), 109028, Moscow, Russia
[d] Centre for Nonlinear Systems, Chennai Institute of Technology, Chennai, 600 044, Tamilnadu, India

ARTICLE INFO

Keywords:
Brusselator
Chaos
Extreme events
Experimental circuit
Phase Slip
Brusselator circuit

ABSTRACT

In this manuscript, we report the rich dynamics of the theoretical Brusselator model, which is driven by a periodic external force. We observed and confirmed a variety of dynamical features with the most interesting extreme events behaviour in the proposed system. The dynamics of the system are characterised by the bifurcation diagram, Lyapunov exponent, phase portraits, and time series segments. The extreme events behaviour is characterised by the probability distribution function, instantaneous phase calculation, and Poincaré return map. Real-time hardware experiments were carried out using an analog electronic circuit, and the outcomes of the experimental observations were confirmed with the numerically obtained results. To the best of our knowledge, we believe that it is for the first time that the occurrence of extreme events has been reported using both the numerical simulation studies and the real-time analog electronic experimental observations on this forced Brusselator chemical model.

1. Introduction

In recent years, there has been a noticeable rise in attention paid to investigating the intricate interplay between the complex dynamics and the chemical systems inherent in oscillating reactions. These studies have revealed various chaotic and non-equilibrium phenomena [1], including mixed mode oscillations [2], complex oscillations, bursting oscillations [3], bistability [4], intermittency, quasichaotic behaviour within the reactions [5] and coupled chemical oscillators [6] revealing intriguing phenomena in the chemical systems [7]. Autocatalytic reactions exert a profound influence on the stability and behaviour of systems, engendering complex dynamics, multiple stable states, and periodic oscillations. These phenomena collectively enrich the captivating realm of chemical kinetics [8] and the exploration of nonlinear reactions [9]. The *Brusselator* is a theoretical chemical model introduced by I. Prigogine and his collaborators [10] to represent autocatalytic chemical reactions with spatial oscillations. It resembles the well-known Belousov–Zhabotinsky (BZ) reaction [11], both exhibiting non-equilibrium behaviour with pattern formation and chemical oscillations. Over the decades, the Brusselator model has been extensively studied, shaping ideas on oscillations and pattern formation far from thermodynamic equilibrium. It is a well-established system in the realm of non-equilibrium instabilities, with numerous research papers dedicated to its exploration, and the model has been subject to extensive investigation, encompassing limit cycles, Turing–Hopf bifurcation [12] and coupled systems [13]. Tomita and his collaborators [14] introduced an external forcing term to the Brusselator model, enabling the study of its response to external perturbations. This addition unveils intriguing and complex dynamics, including the emergence of multistability [15], hysteresis and vibrational resonance [16], controlling chaos [17], non-quantum chirality [18], control of a quasiperiodic route to chaos [19], etc.

Events in dynamical systems that suddenly occur and exhibit an unusual dynamical phenomenon are referred to as rare events or extreme events. Extreme events (EEs) refer to the sudden and random increase in the magnitude of one or more of the state variables of the dynamical system. They encompass a wide range of natural and human-made phenomena, including tsunamis, cyclones, rogue waves [20], earthquakes, droughts [21], chemical explosions, floods [22], stock market fluctuations [23], pandemics [24] and certain transmissible diseases [25]. Despite the low probability of these rare events occurring, their resulting losses can be substantial. The prediction and analysis of extreme events occurring in real-world problems have not been fully mastered

* Corresponding author.
E-mail addresses: maran.cnld@gmail.com (K. Thamilmaran), manimehan@gmail.com (I. Manimehan).

https://doi.org/10.1016/j.chaos.2024.114582
Received 3 October 2023; Received in revised form 1 February 2024; Accepted 6 February 2024
Available online 14 February 2024

yet. Recent studies have delved into understanding the occurrence of such behaviour in dynamical systems [26–29]. Extreme events arising in nonlinear dynamical systems mimic those observed in many physical systems, including fibre optics, nonlinear optics, photonics [30,31], financial systems [32,33], electronic oscillators [34,35], mechanical oscillators [36], chemical oscillators [37] and neural models [38]. While studying nonlinear dynamical systems, the trajectory of a dynamical system typically follows a bounded attractor. Occasionally, they deviate significantly, causing a large magnitude of amplitude, spikes, or bursts due to instability in their state space. These rare occurrences resemble changes in the range of time series produced by the systems, which are often characterised by the large deviations from the nominal behaviour of a system [39]. To confirm these occurrences, specific thresholds are determined by statistical analysis. The study of extreme events in dynamical systems is a growing area of research, as scientists and engineers are interested in understanding the mechanisms that lead to these events and developing methods for predicting them [40], predicting extreme events in dynamical systems is a challenging task, even in deterministic systems. There have been some attempts to find early warnings of extreme events [41,42], but success in this area has been limited so far.

These rare events pose challenges due to limited data, making models more difficult. Developing available mathematical models can help us to understand the mechanisms behind the extreme events and improve our ability to predict and manage them. Conversely, the immediate hardware realisation of the nonlinear circuits capable of producing a variety of chaotic oscillations presents a substantial challenge for the future integration of chaos-based information systems. Notably, the exploration of techniques for generating diverse intricate chaotic oscillations, such as EEs, using uncomplicated electronic devices has attracted considerable theoretical and practical attention. The inquiry into creating the EEs with distinct electrical characteristics is captivating, given their unique nature as electrical signals [34,35]. In continuation of the above, this study places its exclusive emphasis on the emergence of extreme events or occasional large-amplitude oscillations within the Brusselator chemical model when subjected to external periodic perturbations and investigates the dynamical instability causing these events. In the realm of chemical oscillators, only a limited number of experiments have provided evidence of their chaotic nature. To further investigate in the present manuscript the extreme events emerging from the Brusselator chemical model, we have designed a simple analogue electronic circuit and studied their dynamics experimentally in the laboratory. To the best of our knowledge, no prior research has explored this phenomenon within the context of this model or chemical oscillators.

This paper is organised as follows: In Section 2, we introduce the mathematical model of the proposed system and analyse its linear stability. In Section 3, we present the numerical study of the system by varying the system control parameters and also demonstrate the presence of extreme events in this model by representing unusually large events in time series using a qualifying threshold and occasional events in phase space. Further, we have plotted the probability distribution and return map to illustrate the rarity of these events as well as display the phase slips that occur during the extreme events. The global behaviour of the model is studied through the two-parameter bifurcation diagrams, which are given in Section 4. The experimental evidence of extreme events in this model is presented in Section 5. Finally, in Section 6, we draw our conclusions.

2. Mathematical model of brusselator

The *Brusselator* chemical model [10] is a trivial autonomous theoretical oscillator that mimics the autocatalytic reaction. The proposed autonomous *Brusselator* model can be written as,

$$\dot{x} = a - (b+1)x + x^2 y$$
$$\dot{y} = bx - x^2 y, \tag{1}$$

where a and b are constants of system parameters and x and y represent the system state variables of the model (Eq. (1)). Then we have introduced an external periodic forcing term [14] to the Brusselator autonomous model of Eq. (1). The resultant system is a second-order nonautonomous differential equation as follows:

$$\dot{x} = a - (b+1)x + x^2 y + f\sin(\omega t)$$
$$\dot{y} = bx - x^2 y. \tag{2}$$

The system of Eq. (2) is subjected to an external driving force with an amplitude f and frequency ω. Thus, the present model is composed of two simple ordinary differential equations with external forcing, and the resulting oscillations are purely temporal (time-dependent). For understanding the dynamics of our proposed system, we integrated Eq. (2) using the fourth-order Runge–Kutta method with integration time steps $dt = 0.01$, initial condition $x(0) = 0.01$, and $y(0) = 0.02$.

2.1. Linear stability analysis

The stability criterion and the nature of bifurcational analysis on the Brusselator model were reported [10,43]. The equilibrium point for the system Eq. (2) is obtained by setting the derivatives of x and y with respect to time equal to zero and without any external force. The eigenvalues of the system are $\lambda_{1,2} = \frac{1}{2}(-(x^2 + b + 1 - 2xy) \pm \sqrt{(x^2+b+1-2xy)^2 - 4x^2})$. Thus, the system of Eq. (2) has only one equilibrium point, which is (x_0, y_0) = (a, b/a). The eigenvalues at the equilibrium point are $\lambda_{1,2_{equ}} = \frac{1}{2}(-(a^2 - b + 1) \pm \sqrt{(a^2-b+1)^2 - 4a^2})$. The stability of the system depends on the relationship between b and $a^2 + 1$. If $b > (a^2 + 1)$, then $\lambda_{1,2} > 0$, this indicates that the equilibrium point is *unstable*. If $b < (a^2 + 1)$, then $\lambda_{1,2} < 0$, this indicates that the equilibrium point is *stable*. If $b = (a^2 + 1)$, then $\lambda_{1,2} = 0$. This indicates that the equilibrium point is either a *centre* or an *elliptic point*, with oscillatory behaviour. The stability plot for the (a - b) plane for $\lambda_{1,2_{equ}}$ is shown in Fig. 1. The different colour zones are represented by different stability states, say unstable node (USN), unstable focus (USF), stable focus (SF), and stable node (SN). The critical line that represents centre stability is mentioned in an orange line in between USF and SF. From this stability analysis, the system stability changes with respect to parameters a and b since there exists a Hopf bifurcation for $b = a^2 + 1$.

3. Numerical results

To begin with, numerically integrate and analyse the extreme events (EEs) in a system of Eq. (2) by examining its dynamics through a bifurcation diagram depicted in Fig. 2(a) and its corresponding maximum Lyapunov exponent in Fig. 2(b) by varying the system control parameter b within the range of $b \in (1.0, 1.2)$ and chosen the other system parameters are constant as $a = 0.2$, $f = 0.06$, and $\omega = 0.7$ with the initial conditions as $x_0, y_0 = (0.01, 0.02)$. The bifurcation diagram was computed to detect the large peak values of state variable x in each value of the parameter b scanning. To distinguish the extreme events (EEs) from the normal events, a threshold height (H_s) of large amplitude oscillation is determined statistically [44], This statistical approach enables the identification and analysis of the occurrence of EEs in the system. The threshold value H_s is obtained by considering the dynamical aspects of the system observable, which involves measuring the significant large deviations away from the mean value of the state variable of the system. In other words, the EEs are identified as having large amplitudes substantially higher than the average value. The H_s is calculated as follows: $H_s = \langle x_{max} \rangle + n\sigma_{x_{max}}$, where $\langle x_{max} \rangle$ represents the mean of the peak values of state variable x, $\sigma_{x_{max}}$ is the standard deviation of the x_{max}, and n is an integer specific to the system, typically ranging from 4 to 8 for extreme events, whose value determines and distinguishes extreme events from bounded chaos. To calculate H_s for

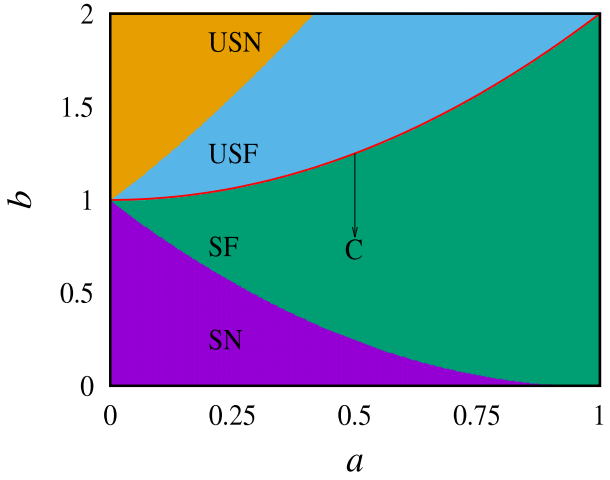

Fig. 1. The stability plot of the equilibrium points in the $(a-b)$ plane for $\lambda_{1,2_{equ}}$ by various values of parameters a and b. Different colours, such the violet for stable node (SN), green for stable focus (SF), sky-blue for unstable focus (USF) and yellow for unstable node (USN), are used to represent different types of stability. (For interpretation of the references to colour in this figure legend, the reader is referred to the web version of this article.)

Table 1
The dynamics of the system (2) are studied by varying the control parameter b, while keeping other system parameters $a = 0.2$, $f = 0.06$, and $\omega = 0.7$ constant.

Range of b	Observed phenomenon
$1.0 < b < 1.0971$	Periodic attractor (PD)
$1.0972 < b < 1.1092$	Bounded chaotic attractor (BC)
$1.1093 < b < 1.1151$	Extreme events for $n = 6$ (EEs)
$1.1093 < b < 1.1214$ $1.1233 < b < 1.1290$ $1.1309 < b < 1.1408$	Extreme events for $n = 4$ (EEs)
$1.1409 < b < 1.2$	Large amplitude chaotic attractor (LAC)

a long run with iterations of 10^8 time units, the system dynamics must be allowed to evolve past transient states. In this Fig. 2(a), we plotted the threshold height H_s for $n = 4$ and $n = 6$. By setting a threshold height, the extreme events can be distinguished from the normal events based on their large amplitudes, with EEs being those peaks that exceed the H_s value. In this one-parameter bifurcation diagram shown in Fig. 2(a), the system undergoes a transition from a regular attractor to a chaotic attractor via the usual period doubling (PD) route. The system's dynamical summary, derived from the bifurcation analysis and accompanied by its corresponding Lyapunov exponents, is presented in Table 1 and shows the ranges within which the system's dynamics exist.

The numerically obtained typical time series $(x(t))$ is shown in Fig. 3(a), and the corresponding phase portrait in the $(x-y)$ plane of the bounded chaotic attractor is depicted in Fig. 3(b) for the value of $b = 1.1092$. In Fig. 3(a) and (b), we observe that the chaotic behaviour remains confined within a specific region, characterised by relatively small amplitudes. Throughout the entire iteration, the system's trajectory shows no evidence of surpassing the threshold value, where we set the basic criterion for extreme events (EEs) as $n = 4$. The threshold value of the bounded chaos for the state variable $x(t)$, calculated from H_s given earlier, is $H_s(n = 4) = 0.4112$ for $b = 1.1092$. Further, in the one-parameter bifurcation diagram of Fig. 2(a), when the control parameter b is varied, we find the occurrence of extreme events embedded in the bounded chaotic attractor. Interestingly, when the parameter b reaches the critical value of 1.1093, there is a sudden chaotic expansion observed in the x_{max} variable. This expansion is substantial enough to surpass the qualifying threshold (H_s) value. This phenomenon has been graphically depicted in Fig. 2(a) (with indicate arrow as EEs) for two distinct scenarios when $n = 4$ (green colour) and $n = 6$ (red colour). The typical extreme events can be clearly seen in the time series plot of the $x(t)$ variable shown in Fig. 3(c) and the corresponding phase portrait in the $(x-y)$ plane (Fig. 3(d)) for the value of $b = 1.1125$. Here, the peaks in the variable $x(t)$ with amplitudes four times and six times as large as the normal amplitudes are observed. In Fig. 3(c) and (d), we observe a significant expansion in the region of bounded chaos. This expansion in the time series exceeds calculated threshold values: $H_s = 1.7763$ for $n = 4$ and $H_s = 2.5012$ for $n = 6$, as indicated by the horizontal dashed red colour line in Fig. 3(c), and this sudden expansion in the system is characterised as an extreme events. As the control parameter b is varied further, the system dynamics bifurcate as non-extreme events with large amplitude chaotic behaviour are indicated as LAC in Fig. 2(a).

3.1. Statistical characterisation

We applied the statistical properties to characterise and confirm the extreme events (EEs) present in the Brusselator system of Eq. (2). In accordance with the findings in Refs. [28,32,45], we have plotted the probability distribution function for the state variable $x(t)$, we have taken the t-span length for a long run with iterations of 2×10^7 time units, allowed the system to evolve past transient states for constant parameters $a = 0.2$, $\omega = 0.7$, $f = 0.06$ and various values of the parameter b and confirmed that the shape of the distribution does not change with respect to the t-span length. Fig. 4(a) shows the PDF for nominal chaos is bounded within a low range of x_{max} values below the H_s mark (vertical dashed black colour line), as expected for $b = 1.1092$, signifying a non-extreme event. Fig. 4(d) reveals a continuously heavy tail distribution, and it surpasses the threshold represented in vertical dotted black colour line. This indicates the occurrence of extreme events, which confirms the low probability of the occurrence of large-amplitude events beyond the H_s mark (vertical black colour line) for $b = 1.1125$, which is calculated for $n = 4$ and $n = 6$ using the respective temporal data.

Further, we have calculated the return map as an additional tool for differentiating the bounded chaotic (BC) oscillations from the extreme events (EEs) oscillations. In Fig. 4(b), (e), we plotted the Poincaré return map, which is obtained by plotting the first peak values $x_{\max_n}$ against the next peak values $x_{\max_{n+1}}$ for the system (2). We observe a distinct behaviour in the bounded chaos for $b = 1.1092$, where the return map remains locked and does not cross the H_s (plotted as a dashed red line). This confinement to the bounded region signifies the presence of non-extreme events, as shown in Fig. 4(b). Interestingly, as we change the parameter towards $b = 1.1125$, we notice a significant increase in amplitude of x_{max}, leading to large events that cause the return map points to exceed the H_s (exceeding points are plotted as red hollow circles and H_s as a dashed red line). This crucial observation validates the existence of extreme events in system Eq. (2), as shown in Fig. 4(e). In addition, we plotted a projection of 3D phase plots in Fig. 4(c) and (f) to illustrate how the system transitions from bounded chaos (Fig. 4(c)) to extreme events (Fig. 4(f)) by including the external periodic force $\sin(\omega t)$ as the third axis, and Fig. 4(f) represents the events that cross the threshold H_s indicated in red colour.

To better understand the system's behaviour, we applied a Hilbert transform to the variable $x(t)$ and an external periodic signal $\sin(\omega t)$ as the third axis, as Fig. 4(f) represents. This allowed us to determine their instantaneous phase and subsequently find the difference between these instantaneous phases, thus calculating the phase difference $\delta\phi$. During the bounded chaos, we observed that the system remained phase-locked to the external periodic force. However, during the occurrence of large events, particularly extreme events, phase slips were found to occur because the system temporarily lost its phase-locking to the external periodic force, leading to a sudden and transient shift in its phase, which is shown in Fig. 5.

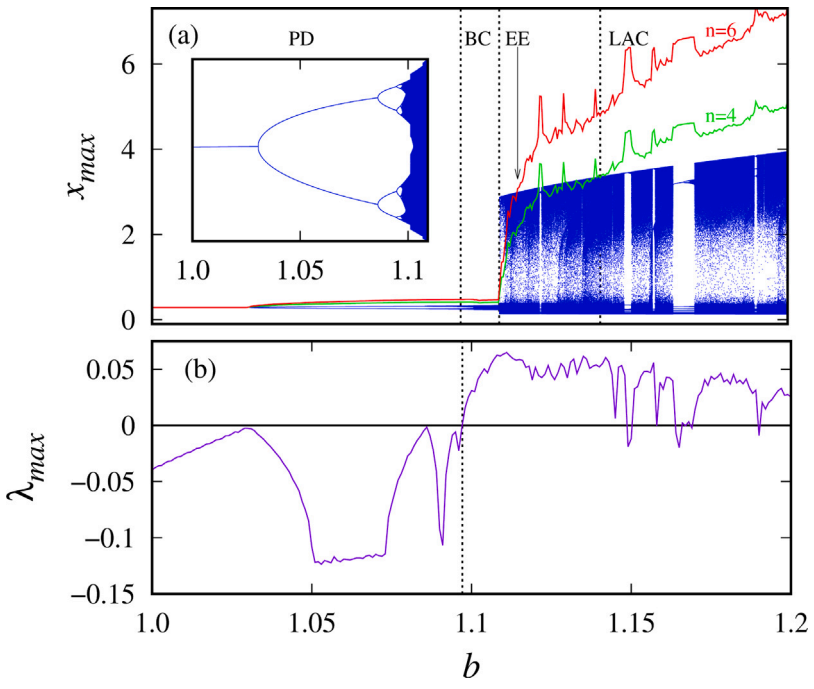

Fig. 2. (a) One-parameter bifurcation diagram in the $(b - x_{max})$ plane. The blue dot represents the maxima (x_{max}) of the state variable x. The green and red colour lines for $n = 4$ and $n = 6$ respectively, show the critical threshold value calculated from $H_s = \langle x_{max} \rangle + n\sigma_{x_{max}}$ for identifying the extreme events. (b) corresponding maximum Lyapunov exponent in the $(b - \lambda_{max})$ plane. The other system parameters are $a = 0.2$, $f = 0.06$, and $\omega = 0.7$ constant. (For interpretation of the references to colour in this figure legend, the reader is referred to the web version of this article.)

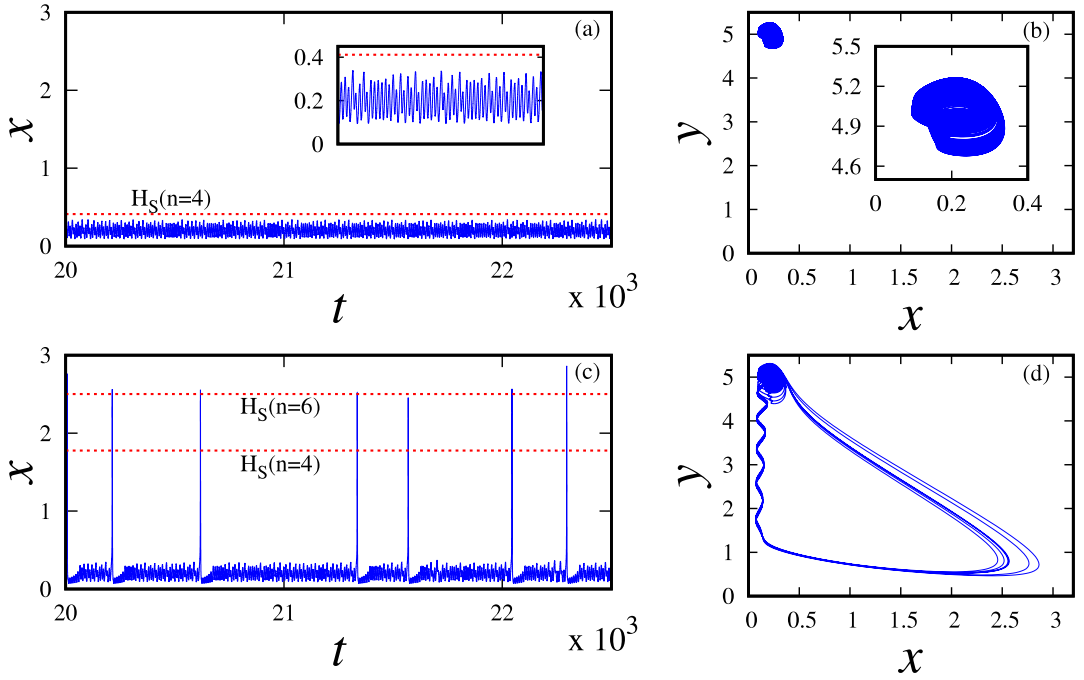

Fig. 3. (online colour) The left and right panels display the time evolution of the state variable $x(t)$ and the corresponding typical phase portraits in the $(x - y)$ planes, respectively. (a) and (b) demonstrate the emergence of non-extreme events for $b = 1.1092$; (c) and (d) the extreme events for $b = 1.1125$ with constant parameter values $a = 0.2$, $\omega = 0.7$, and $f = 0.06$. Here, the horizontal dashed red lines represents the threshold height H_s for $n = 4$ and $n = 6$.

4. Two parameter bifurcation

The overall system dynamics across the parameter space $(a - b)$ were depicted in Fig. 6, where $a \in [0,\ 0.28]$ and $b \in [1.05,\ 1.5]$. Our focus is to identify and distinguish the regions of extreme events (EEs) from non-extreme events (NEEs). To begin with, we found that the EEs are exhibited when the system demonstrates chaotic behaviour. Hence, to distinguish the EEs region from the other region as a function of the parameters a and b, we estimated the threshold height (H_s). For a long run with iterations of 10^8 time units, if the system shows nominal chaos with the maximum values of the x-variable (x_{max}) exceeding a threshold height for $n = 4$, then the dynamics in that specific region are marked as EEs (represented by the red colour points in Fig. 6(a). Conversely, if the system does not surpass H_s, then these parameter values are marked

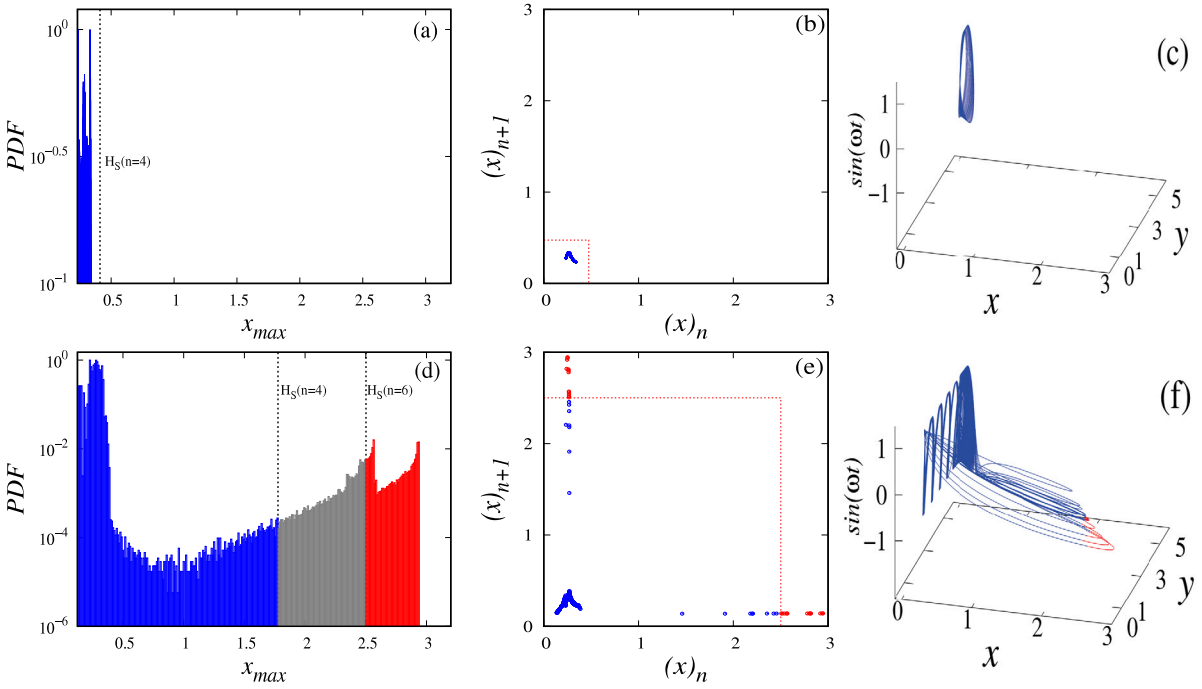

Fig. 4. (online colour) The left panel displays the probability distribution function (PDF). The middle panel displays Poincaré return map in the $(x_n - x_{n+1})$ plane, and the right panel shows the projection of 3D phase plots, where the third axis represents the external periodic force sin(ωt). For bounded chaos ((a)–(c)), $b = 1.1092$ and for extreme events ((d)–(f)), $b = 1.1125$.

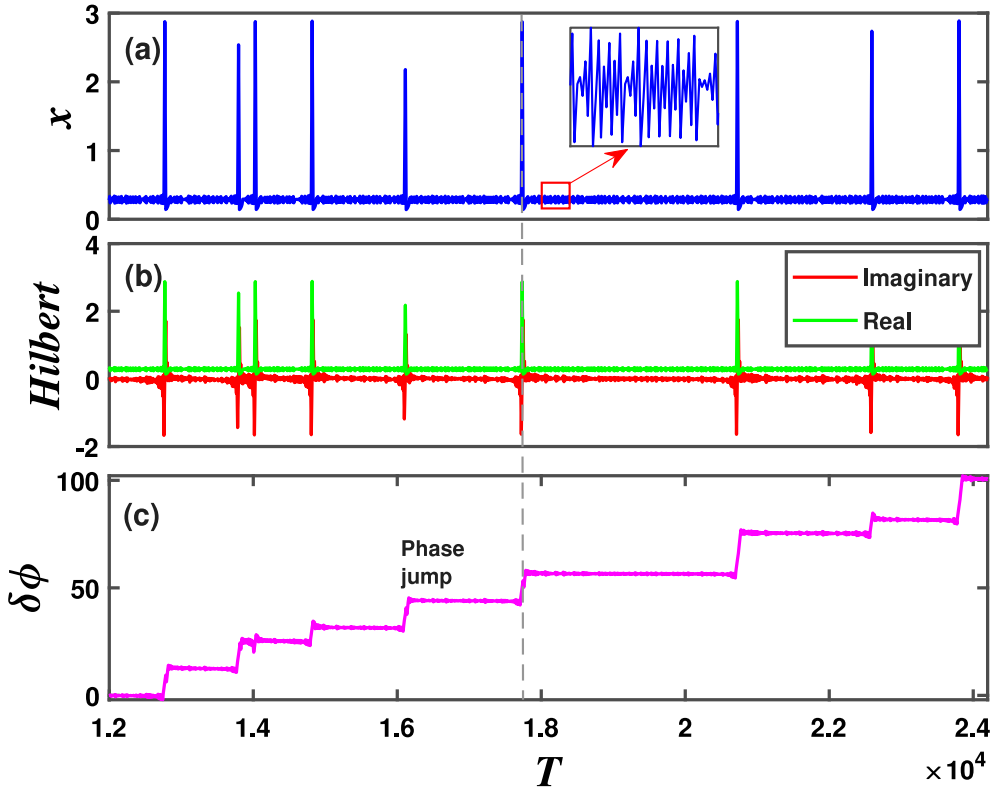

Fig. 5. Instantaneous phase slips analysis for the extreme events data for $b = 1.1125$. (a) EEs time series of the $x(t)$ variable; (b) Hilbert transformed signals real (green) and imaginary (red colour); and (c) phase slips analysis for the same time duration. The vertical grey dashed line demonstrates the slips at extreme events. (For interpretation of the references to colour in this figure legend, the reader is referred to the web version of this article.)

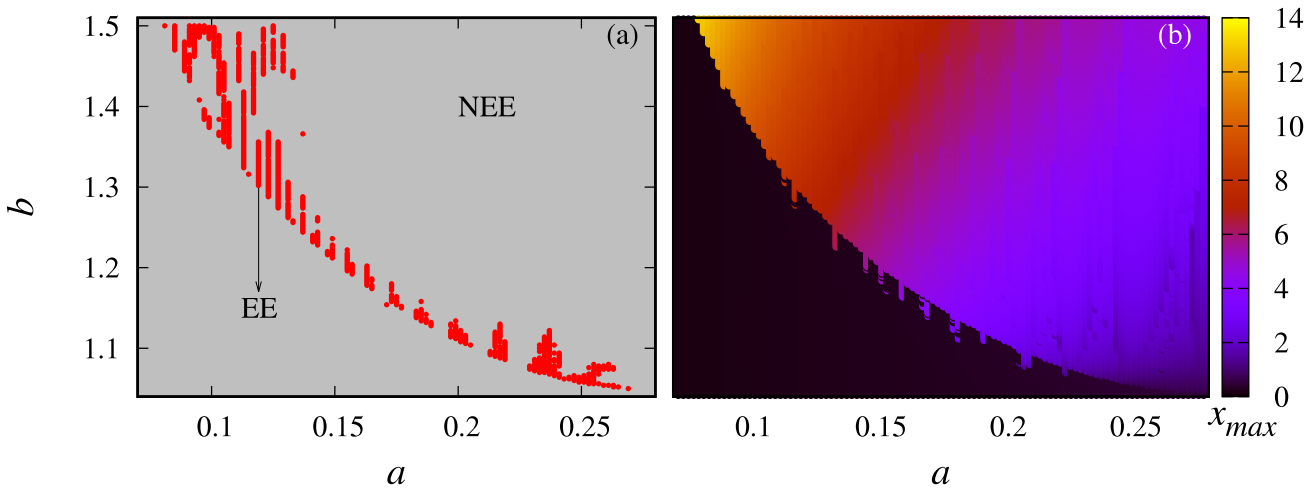

Fig. 6. The two-parameter diagram in the parameter space of (a, b) for (a) threshold value (H_s), where the red colour points represents the parameter values for the existence of EEs, the grey colour point indicates the NEEs states and (b) x_{max} demonstrates the emergence of distinct states. (For interpretation of the references to colour in this figure legend, the reader is referred to the web version of this article.)

as part of the non-extreme events region (represented by grey colour points in Fig. 6(a). Throughout this analysis, we verified the emergence of these extreme events within the specified parameter ranges of a and b using time series data and one-parameter bifurcation diagrams. To confirm this with a two-parameter bifurcation for x_{max} depicted in Fig. 6(b), the dark region indicates a low height amplitude of the state variable x_{max}, suggesting the presence of periodic oscillations and bounded chaos in those regions. On the other hand, the colour gradient from violet to yellow represents high amplitudes of x_{max}. These high amplitudes indicate the occurrence of expansion in x_{max}. From Figs. 6(a) and 2(a), we can deduce that extreme events are found to be present only at the initial stage of the sudden expansion of x_{max}. As time progresses, the amplitudes tend to fall more frequently, leading them to no longer qualify as extreme events. Figs. 6(a) and (b), it is evident that in the region where parameter $a \in (0, 0.13)$ and $b \in (1.3, 1.5)$, there is a noticeable presence of high amplitudes (red–yellow colour) of x_{max} and a high probability of extreme events occurring in this range.

5. Experimental observations of extreme events

Recently, experimental circuit implementation has offered an alternative avenue to investigate or verify the feasibility of physical implementations of theoretical dynamical models and to apply them in practical scenarios. To analyse the circuit dynamics and compare them with the numerical studies of a normalised model, it is derived by performing circuit variable substitutions and parameter transformations [35]. Therefore, in this section, we have designed a simple analog circuit and implemented it in the laboratory to validate the obtained numerical results of the two-dimensional nonautonomous Brusselator model given in the Eq. (2) described earlier. According to the above numerical analysis, Fig. 7 shows the schematic of experimental circuit realisation in the top panel, and the complete analog circuit assembled using readily available discrete components was utilised to build the proposed chaotic circuit of the Brusselator model of Eq. (2), which is shown on a breadboard in the bottom panel. The resulting circuit is straightforward, cost-effective, and can also serve laboratory experiments and educational purposes for exploring the innovative effects in the dynamics of complex classical oscillators, as mentioned earlier. This circuit consists of linear resistors, capacitors, and μA741C operational amplifiers. The nonlinear functions in Eq. (2) are generated by using AD633JN analog multipliers. The operational amplifiers and multipliers operate with supply voltages of ±12 V and saturated voltages of ±9.5 V. The arbitrary waveform generator (Agilent 33500B) is taken as the external periodic forcing voltage source $f(t) = F sin(\Omega t)$.

By applying Kirchhoff's circuit laws to the designed circuit (top panel) of Fig. 7, we get the following circuital equations:

$$\frac{dv_{C_1}}{dt} = \frac{1}{R_4C_1}E - \frac{1}{R_1C_1}v_{C_1} + \frac{0.01}{R_2C_1}v_{C_1}^2 v_{C_2} + \frac{1}{R_4C_1}F sin(\Omega t), \tag{3}$$

$$\frac{dv_{C_2}}{dt} = \frac{1}{R_6C_2}v_{C_1} - \frac{0.01}{R_5C_2}v_{C_1}^2 v_{C_2}. \tag{4}$$

Here, v_{C_1} and v_{C_2} are the voltages developed across the capacitors C_1 and C_2 respectively, represented by the circuit state variables.

Similar to the numerical simulation studies in Section 3, we have observed the occurrence of EEs and bounded chaos followed by the period doubling route in experimentally also and the values of various circuit components are pre-determined in the circuit depicted in Fig. 7. For this breadboard experiment, specific circuit component values can be chosen using an appropriate time scale [34]. The circuit's time-constant-related circuit elements have been optimised to $R = 100$ kΩ and $C = 2.2$ nF. Further, we have fixed the values of other circuit elements as follows: The capacitance values of the capacitors are fixed as $C_1 = C_2 = 2.2$ nF. The resistances of resistors are set as follows: $R_1, R_3, R_6, R_7, R_8 = 10$ kΩ, $R_2 = 6.8$ kΩ, $R_5 = 3.3$ kΩ, and $R_4 = 100$ kΩ. The amplitude $F = 4.5$ V and frequency $\Omega = 6.2$ kHz of the external periodic voltage source. The gains of the analog multipliers M_1 and M_2 are $(1/10)$ V. It is worth noting that all the circuit components have tolerances of ±5 %. Also, we varied the resistance values of R_4 and R_6 in the breadboard circuit during the experimental observations and to match the selected control parameters a and b, as specified in Eq. (2), based on the results of numerical simulation studies.

Specifically, in the laboratory experiments, a precision potentiometer is utilised for the adjustable feedback resistor R_4 in the first integrator (IC1) of the circuit (Fig. 7 (top panel), which is considered the control parameter. The tunable potentiometer has a resistance of 100 kΩ to adjust the external bias (E) in the experimental observations. The choice of these values is justified by our wish to use the same sets of system parameters for both numerical and experimental studies. The resistance of the variable resistor R_4 is gradually tuned; for different values of R_4, the circuit generates different attractors experimentally.

In order to begin our experimental study, in Fig. 7, when the resistance R_4 is set to 22.5 kΩ, the oscillator generates periodic limit cycle oscillations. When the control parameter R_4 is varied in the range of (23 kΩ $\leq R_4 \leq$ 55.5 kΩ), we observed the period-doubling

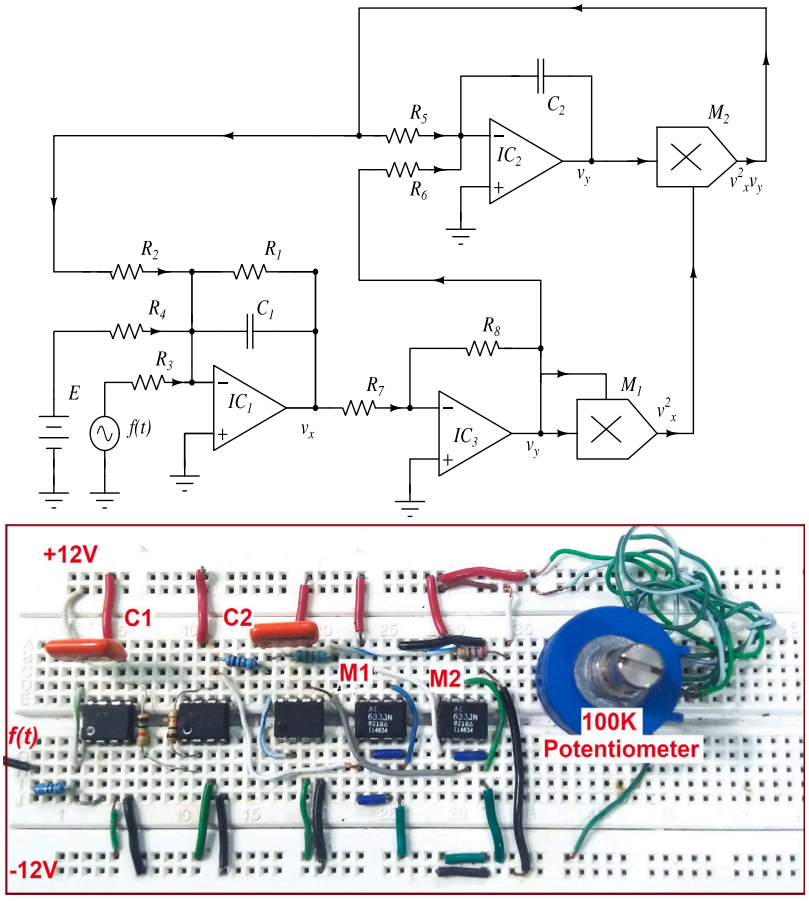

Fig. 7. (online colour) A schematic diagram of analog electronic circuit realisation (top panel) and the corresponding analog circuit is implemented on a breadboard (bottom panel) of the Brusselator model of Eq. (2).

sequences; the range (55.5 kΩ ≤ R_4 ≤ 78.0 kΩ), chaotic regime, and the range (78.0 kΩ ≤ R_4 ≤ 82.6 kΩ), extreme events oscillations. The experimentally observed results are summarised in Fig. 8. Snapshots of the experimental time series and phase portraits are captured using the analog oscilloscope for different values of the circuit control parameter, the variable resistance R_4. The experimental circuit outputs can directly be displayed on an oscilloscope by feeding the output voltages v_{C_1} and v_{C_2} to connect them to the X and Y channels of the dual-channel analog oscilloscope (ScientiFic SM 410) with 1 V/div in the X direction and 1 V/div in the Y direction. The experimentally obtained time series of voltage $v_{C_1}(t)$ (Fig. 8a(i)) and corresponding the typical phase portrait of bounded chaotic attractor in the $(v_{C_1} - v_{C_2})$ plane (Fig. 8a(ii)) for $R_4 = 56.5$ kΩ. Continuing to vary the resistance R_4 in the range of R_4 (78.0 kΩ, 83.0 kΩ), we observe the occurrence of extreme events embedded within the bounded chaotic attractor, as shown in Fig. 8(b). The temporal time evolution plot for the voltage $v_{C_1}(t)$ and corresponding the typical phase portrait of extreme events in the $(v_{C_1} - v_{C_2})$ plane for $R_4 = 80.5$ kΩ as shown in Fig. 8b(i) and b(ii). Obviously, the experimentally captured results of chaotic behaviour and extreme events oscillations agree with those shown in Fig. 3 by the numerical simulations.

6. Conclusion

In this article, we have presented the dynamics of a Brusselator chemical system driven by an external periodic force, studied both numerically and experimentally. We have investigated and confirmed many dynamical phenomena, including the well-known period doubling, chaotic oscillations, and the most intriguing extreme events behaviour in the proposed chemical model. The one-parameter bifurcation diagram, maximum Lyapunov exponent, phase portraits, and time series segments characterise the system's dynamics, while the probability distribution function, the instantaneous phase calculation, and the Poincaré return map characterise the extreme events behaviour. Additionally, a two-parameter bifurcation diagram is used to distinguish extreme events within a two-parameter space. Further, the real-time hardware analog electronic experiments were carried out in the laboratory, and the findings confirmed the numerically obtained results. To the best of our knowledge, this is the first analog electronic experimental study on the Brusselator chemical model with the observation of extreme events. These results are giving more insight into how to construct real-time experiments with chemical reaction setups and avoid external stimuli. The system creates intermittency peaks [46] and multistability [47]. However, in our work, we have reported that external periodic forces cause very large oscillations and lead to extreme events for appropriate system parameter regimes. Adding the external periodic force to the Brusselator mathematical model is an initial assumption, and it helps to understand the real chemical experiments for the Brusselator autocatalytic reaction. The external periodic force has been applied to the state variable x. The autocatalytic nature of the system is evident in the state variables x and y, which evolve chaotically with extreme event oscillations. However, due to the addition of the external periodic force, the dimensions are increased, resulting in chaotic oscillations with rich dynamical behaviours. These intriguing results, such as extreme events and reverse period doubling, will be replicated in real Brusselator experiments to uncover the hidden dynamics in the near future.

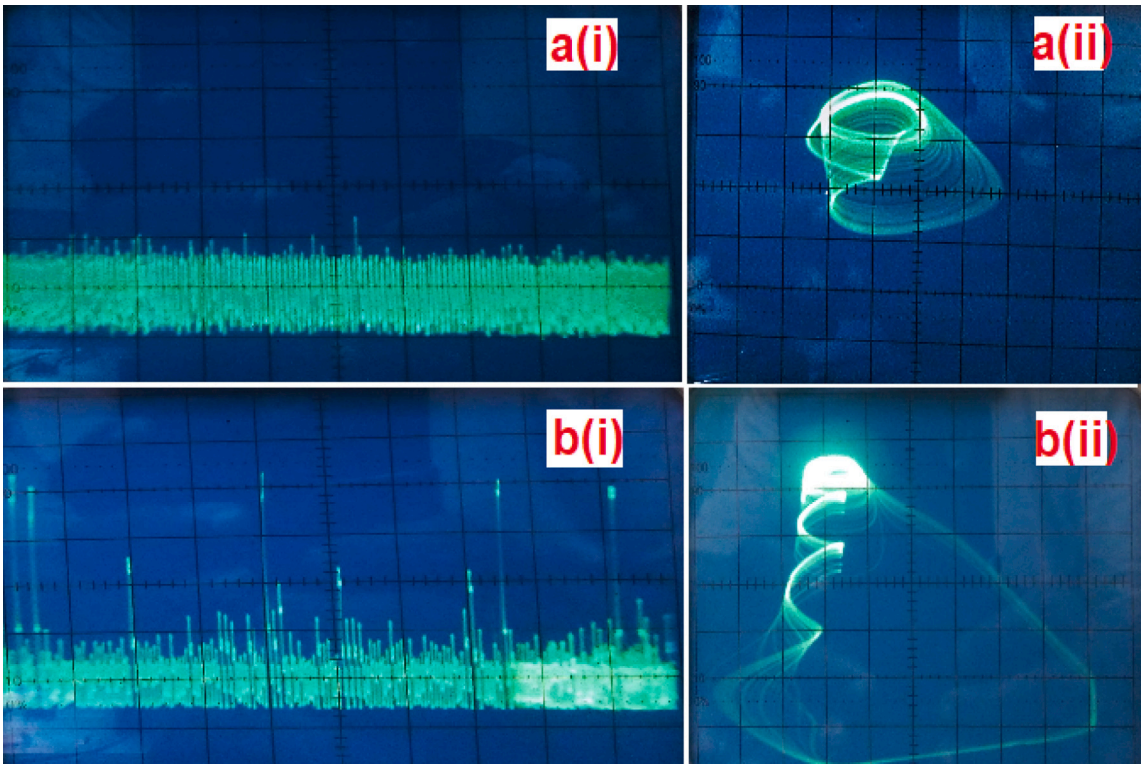

Fig. 8. (online colour) Experimentally captured (i) the temporal time evolutions of $v_{C1}(t)$ (horizontal axis 0.5 ms, vertical axis 0.5 mV/div) and (ii) the phase portraits in the $(v_{C_1} - v_{C_2})$ plane of Brusselator model (horizontal axis 0.5 mV/div, vertical axis 0.5 mV/div). (a) bounded chaotic attractor for $R_4 = 5.65$ kΩ and (b) extreme events for $R_4 = 8.76$ kΩ.

CRediT authorship contribution statement

S.V. Manivelan: Writing – original draft, Visualization, Software, Resources, Methodology, Investigation, Formal analysis, Data curation. **S. Sabarathinam:** Writing – review & editing, Writing – original draft, Visualization, Validation, Supervision, Project administration, Methodology, Investigation, Formal analysis. **K. Thamilmaran:** Visualization, Validation, Supervision, Software, Resources, Formal analysis, Data curation, Conceptualization. **I. Manimehan:** Writing – review & editing, Writing – original draft, Supervision, Conceptualization.

Declaration of competing interest

The authors declare that they have no known competing financial interests or personal relationships that could have appeared to influence the work reported in this paper.

Data availability

Data will be made available on request.

Acknowledgement

K.T. acknowledges the Chennai Institute of Technology, India, which provided support under the following funding number: CIT/CCM/2023/RP-013, for its experimental and computational assistance. SS acknowledges the Basic Research Program of the National Research University, Higher School of Economics, Moscow.

References

[1] Scott SK. Chemical chaos, vol. 24, Oxford University Press; 1993.
[2] Petrov V, Scott SK, Showalter K. Mixed-mode oscillations in chemical systems. J Chem Phys 1992;97:6191–8.
[3] Chen J, Li X, Hou J, Zuo D. Bursting oscillation and bifurcation mechanism in fractional-order brusselator with two different time scales. J Vibroeng 2017;19:1453–64.
[4] Vellela M, Qian H. Stochastic dynamics and non-equilibrium thermodynamics of a bistable chemical system: the schlögl model revisited. J R Soc Interface 2009;6:925–40.
[5] Bodale I, Oancea VA. Chaos control for willamowski–rössler model of chemical reactions. Chaos Solitons Fractals 2015;78:1–9.
[6] Dolnik M, Epstein IR. Coupled chaotic chemical oscillators. Phys Rev E 1996;54:3361.
[7] Epstein IR, Pojman JA. An introduction to nonlinear chemical dynamics: oscillations, waves, patterns, and chaos. Oxford University Press; 1998.
[8] Kannan KS, Ansari MAT, Amutha K, Chinnathambi V, Rajasekar S. Control of chaos and bifurcation by nonfeedback methods in an autocatalytic chemical system. Int J Chem Kinet 2023;55:261–7.
[9] Owolabi KM, Agarwal RP, Pindza E, Bernstein S, Osman MS. Complex turing patterns in chaotic dynamics of autocatalytic reactions with the caputo fractional derivative. Neural Comput Appl 2023;1–27.
[10] Prigogine I, Lefever R. Symmetry breaking instabilities in dissipative systems. ii. J Chem Phys 1968;48:1695–700.
[11] Levenspiel O. Chemical reaction engineering. John wiley & sons; 1998.
[12] De Wit Anne, Lima Diana, Dewel Guy, Borckmans Pierre. Spatiotemporal dynamics near a codimension-two point. Phys Rev E 1996;54(1):261.
[13] Yu P, Gumel A. Bifurcation and stability analyses for a coupled brusselator model. J Sound Vib 2001;244:795–820.
[14] Tomita K, Kai T, Hikami F. Entrainment of a limit cycle by a periodic external excitation. Progr Theoret Phys 1977;57:1159–77.
[15] Rech PC. Multistability in a periodically forced brusselator. Braz J Phys 2021;51:144–7.
[16] Guruparan S, Nayagam BRD, Ravichandran V, Chinnathambi V, Rajasekar S. Hysteresis, vibrational resonance and chaos in brusselator chemical system under the excitation of amplitude modulated force. Chem Sci Rev Lett 2015;4:870–9.
[17] Sanayei A. Controlling chaotic forced brusselator chemical reaction. In: Proceedings of the world congress on engineering. Vol. 3, 2010.
[18] Gallas JA. Non-quantum chirality in a driven brusselator. J Phys: Condens Matter 2022;34:144002.
[19] Chakravarti S, Marek M, Ray W. Reaction–diffusion system with brusselator kinetics: Control of a quasiperiodic route to chaos. Phys Rev E 1995;52:2407.
[20] Pelinovsky E, Kharif C, et al. Extreme ocean waves, vol. 1495, Springer; 2008.
[21] Webb GR. Sociology, disasters, and terrorism: Understanding threats of the new millennium. Sociol Focus 2002;35:87–95.

[22] Sornette D. Critical phenomena in natural sciences: chaos, fractals, selforganization and disorder: concepts and tools. Springer Science & Business Media; 2006.
[23] Johansen A, Sornette D, et al. Shocks, crashes and bubbles in financial markets. Bruss Econ Rev 2010;53:201–53.
[24] Varshney V, Singh A, Kumarasamy S, Mishra A, Srinivasan S. Effect and importance of artificial extreme event in indian covid-19 vaccination data sets. In: AIP conference proceedings, vol. 2768, AIP Publishing; 2023.
[25] Mack A, Choffnes ER, Hamburg MA, Relman DA, et al. Global climate change and extreme weather events: Understanding the contributions to infectious disease emergence: Workshop summary. National Academies Press; 2008.
[26] Ray A, Bröhl T, Mishra A, Ghosh S, Ghosh D, Kapitaniak T, Dana SK, Hens C. Extreme events in a complex network: Interplay between degree distribution and repulsive interaction. Chaos 2022;32.
[27] Milovanov AV, Rasmussen JJ, Groslambert B. Black swans, extreme risks, and the e-pile model of self-organized criticality. Chaos Solitons Fractals 2021;144:110665.
[28] Kumarasamy S, Srinivasan S, Gogoi PB, Prasad A. Emergence of extreme events in coupled systems with time-dependent interactions. Commun Nonlinear Sci Numer Simul 2022;107:106170.
[29] Sudharsan S, Venkatesan A, Muruganandam P, Senthilvelan M. Suppression of extreme events and chaos in a velocity-dependent potential system with time-delay feedback. Chaos Solitons Fractals 2022;161:112321.
[30] Akhmediev N, Kibler B, Baronio F, Belić M, Zhong W-P, Zhang Y, Chang W, Soto-Crespo JM, Vouzas P, Grelu P, et al. Roadmap on optical rogue waves and extreme events. J Opt 2016;18:063001.
[31] Tlidi M, Taki M. Rogue waves in nonlinear optics. Adv Opt Photonics 2022;14:87–147.
[32] Thangavel B, Srinivasan S, Kathamuthu T, Zhai G, Gunasekaran N. Dynamical analysis of t–s fuzzy financial systems: A sampled-data control approach. Int J Fuzzy Syst 2022;24:1944–57.
[33] Gilli M, Këllezi E. An application of extreme value theory for measuring financial risk. Comput Econ 2006;27:207–28.
[34] Kingston SL, Thamilmaran K, Pal P, Feudel U, Dana SK. Extreme events in the forced liénard system. Phys Rev E 2017;96:052204.
[35] Thangavel B, Srinivasan S, Kathamuthu T. Extreme events in a forced bvp oscillator: Experimental and numerical studies. Chaos Solitons Fractals 2021;153:111569.
[36] Kaviya B, Gopal R, Suresh R, Chandrasekar V. Route to extreme events in a parametrically driven position-dependent nonlinear oscillator. Eur Phys J Plus 2023;138:36.
[37] Tlidi M, Gandica Y, Sonnino G, Averlant E, Panajotov K. Self-replicating spots in the brusselator model and extreme events in the one-dimensional case with delay. Entropy 2016;18:64.
[38] Roy A, Sinha S. Impact of coupling on neuronal extreme events: Mitigation and enhancement. Chaos 2023;33.
[39] Cavalcante HLdS, Oriá M, Sornette D, Ott E, Gauthier DJ. Predictability and suppression of extreme events in a chaotic system. Phys Rev Lett 2013;111:198701.
[40] Chowdhury SN, Ray A, Dana SK, Ghosh D. Extreme events in dynamical systems and random walkers: A review. Phys Rep 2022;966:1–52.
[41] Farazmand M, Sapsis TP. Dynamical indicators for the prediction of bursting phenomena in high-dimensional systems. Phys Rev E 2016;94:032212.
[42] Zamora-Munt J, Garbin B, Barland S, Giudici M, Leite JRR, Masoller C, Tredicce JR. Rogue waves in optically injected lasers: Origin, predictability, and suppression. Phys Rev A 2013;87:035802.
[43] Nicolis G, Prigogine I. Self-organization in nonequilibrium systems: from dissipative structures to order through fluctuations. A wiley-interscience publication, Wiley; 1977, URL: https://books.google.ru/books?id=mZkQAQAAIAAJ.
[44] Massel SR. Ocean surface waves: their physics and prediction, vol. 11, World scientific; 1996.
[45] Bhagyaraj T, Sabarathinam S, Popov V, Thamilmaran K, Vadivel R, Gunasekaran N. Fuzzy sampled-data stabilization of hidden oscillations in a memristor-based dynamical system. Int J Bifurcation Chaos 2023;33:2350130.
[46] Chen S-G, Hao B-L, Wang G-R. Intermittent chaos in the forced brusselator. Acta Phys Sin 1984;32:1139–48.
[47] Kolinichenko A, Ryashko L. Multistability and stochastic phenomena in the distributed brusselator model. J Comput Nonlinear Dyn 2020;15:011007.